Gain margins and phase margins for sampled-data control systems with adjustable parameters

C.-H. Chang, MS
Prof. K.-W. Han, PhD

Indexing terms: Control systems, Mathematical techniques

Abstract: This paper presents a method for finding the boundaries of constant gain margin and phase margin of sampled-data control systems. The considered systems are first modified by adding a gain-phase margin tester, then the characteristic equations are formulated and factored into stability equations, and finally the parameter-plane method is used to find the boundaries of constant gain margin and phase margin. The main advantage of the presented method is to obtain complete information about the effects of adjustable and/or variable parameters on gain margins and phase margins.

1 Introduction

For the analysis and design of practical control systems, gain margin and phase margin are the two important specifications. The frequency domain approach, based upon the works of Nyquist, Bode and Nichols, permits a designer to find these two values in a simple manner [1]. However, this approach is not suitable for systems with two or more adjustable parameters. On the other hand, the Vishnegradskii diagram [2], the parameter-plane method [3, 4], the stability-equation method [5, 6] are all useful for plotting the stability boundaries, the damping ratio boundaries, etc., and for finding the effects of parameter variations, but no result related to phase margin and gain margin has been given.

In References 7 and 8, methods of plotting the boundaries of constant gain margin and phase margin in a parameter plane or a parameter space have been proposed for analysis and design of continuous control systems and systems with multiple transport lags. The main purpose of this paper is to extend the aforementioned papers to plot the boundaries of constant gain margin and phase margin of sampled-data control systems.

The advantage of the proposed method is that the design work by adjusting parameters to obtain desirable gain margin and phase margin can be simplified due to the fact that the effects of parameter variations on phase margin and gain margin can be clearly defined. In addition, the phase crossover frequency and the gain crossover frequency can be obtained directly from these boundaries.

The presented method is useful for analysis and design of very complicated systems. A nonminimum phase sampled-data control system with multiple gain margins and phase margins is presented as an illustration.

Paper 7544D (C8), first received 7th August and in revised form 20th December 1989

C.-H. Chang is with the Institute of Electronics, National Chiao-Tung University, Taiwan, Republic of China

Prof. Han is Project Director, Center of System Development, Chung-Shan Institute of Science and Technology, and Adjunct Professor, National Chiao-Tung University, Taiwan, Republic of China

2 Basic approach

Consider the system shown in Fig. 1. The open-loop transfer function is

$$G(z) = \frac{N(z)}{D(z)} \tag{1}$$

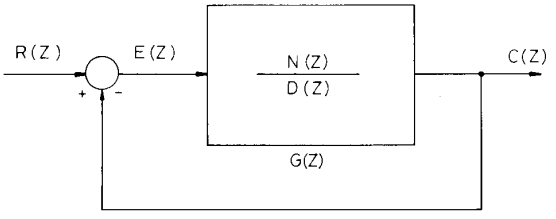

Fig. 1 *Block diagram of a sampled-data control system*

where $z = e^{sT}$, and T is the sampling period. Let $s = j\omega$, then one has

$$z = e^{j\omega T} = \cos \omega T + j\sqrt{(1 - \cos^2 \omega T)} \tag{2}$$

Define $\omega_z = \cos \omega T$, then eqn. 2 becomes

$$z = \omega_z + j\sqrt{(1 - \omega_z^2)} \tag{3}$$

Substituting eqn. 3 into eqn. 1 yields

$$G(z) = \text{Re } [G(z)] + j \text{ Im } [G(z)] \tag{4}$$

where Re $[G(z)]$ and Im $[G(z)]$ are the real and imaginary parts of $G(z)$, respectively. Eqn. 4 can be expressed in terms of its magnitude and phase such as

$$G(z) = |G(z)| e^{j\phi} \tag{5}$$

where

$$|G(z)| = \sqrt{[\text{Re } G(z)]^2 + \text{Im } [G(z)]^2} \tag{6}$$

and

$$\phi = \underline{/G(z)} = \tan^{-1} \frac{\text{Im } [G(z)]}{\text{Re } [G(z)]} \tag{7}$$

From eqns. 1 and 5, one has

$$D(z)\,|\,G(z)\,|\,e^{j\phi} - N(z) = 0 \tag{8}$$

i.e.,

$$D(z) - \frac{1}{|\,G(z)\,|e^{j\phi}}\,N(z) = 0 \tag{9}$$

Define

$$1/|\,G(z)\,| = A \tag{10a}$$

$$\phi + 180^\circ = \Theta \tag{10b}$$

Then, eqn. 9 becomes

$$D(z) + Ae^{-j\Theta}N(z) = 0 \tag{11}$$

Note that A is the gain margin of the system if $\Theta = 0$, and that Θ is the phase margin of the system if $A = 1$. This can be checked by use of a Nyquist plot. The physical meaning of eqn. 11 is that the gain margin and the phase margin of a system can be determined by the gain-phase margin tester $Ae^{-j\Theta}$ which can be considered as an additional block as shown in Fig. 2.

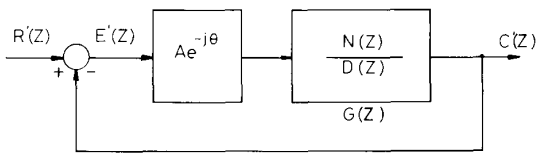

Fig. 2 *A control system with a gain-phase margin tester*

Eqn. 11 can also be considered as

$$F(z,\, Ae^{-j\Theta}) = 1 + Ae^{-j\Theta}G(z) = 0 \tag{12}$$

which indicates that the gain margin and the phase margin of the system can be determined from the characteristic equation of the system with a gain-phase margin tester.

Rewrite eqn. 12 as

$$F(z,\, Ae^{-j\Theta}) = D(z) + Ae^{-j\Theta}N(z) = \sum_{k=0}^{n} a_k(z)z^k = 0 \tag{13}$$

where the coefficients $a_k(z)$ are functions of $Ae^{-j\Theta}$ and the system parameters, and can be defined in the following manner in order to include all possible linear combinations of parameters:

$$a_k(z) = \alpha b_k + \alpha Ae^{-j\Theta}c_k + \beta d_k + \beta Ae^{-j\Theta * e_k} + f_k + Ae^{-j\Theta}g_k \tag{14}$$

where α and β are parameters.

Since $z = \omega_z + j\sqrt{(1-\omega_z^2)}$ as defined in eqn. 3, one has

$$z^k = [T_k(\omega_z) + j\sqrt{(1-\omega_z^2)}U_k(\omega_z)] \tag{15}$$

where $T_k(\omega_z)$ and $U_k(\omega_z)$ are the Chebyshev functions of the first and second kinds, respectively. The argument of Chebyshev functions is $0 \leqslant |\,\omega_z\,| \leqslant 1$, and can be calculated by applying the recurrence formulae

$$T_{k+1}(\omega_z) - 2\omega_z T_k(\omega_z) + T_{k-1}(\omega_z) = 0 \tag{16a}$$

$$U_{k+1}(\omega_z) - 2\omega_z U_k(\omega_z) + U_{k-1}(\omega_z) = 0 \tag{16b}$$

where $T_0(\omega_z) = 1$, $T_1(\omega_z) = \omega_z$, $U_0(\omega_z) = 0$ and $U_1(\omega_z) = 1$.

Substituting eqns. 14 and 15 into eqn. 13 gives

$$F(\omega_z, A, \Theta) = [\alpha B_1(\omega_z, A, \Theta) + \beta C_1(\omega_z, A, \Theta) + D_1(\omega_z, A, \Theta)] + j[\alpha B_2(\omega_z, A, \Theta) + \beta C_2(\omega_z, A, \Theta) + D_2(\omega_z, A, \Theta)] \tag{17}$$

where

$$B_1 = \sum_{k=0}^{n} \{T_k(\omega_z)b_k + Ac_k[T_k(\omega_z)\cos\Theta + \sqrt{(1-\omega_z^2)}U_k(\omega_z)\sin\Theta]\} \tag{18a}$$

$$C_1 = \sum_{k=0}^{n} \{T_k(\omega_z)d_k + Ae_k[T_k(\omega_z)\cos\Theta + \sqrt{(1-\omega_z^2)}U_k(\omega_z)\sin\Theta]\} \tag{18b}$$

$$D_1 = \sum_{k=0}^{n} \{T_k(\omega_z)f_k + Ag_k[T_k(\omega_z)\cos\Theta + \sqrt{(1-\omega_z^2)}U_k(\omega_z)\sin\Theta]\} \tag{18c}$$

$$B_2 = \sum_{k=0}^{n} \{U_k(\omega_z)\sqrt{(1-\omega_z^2)}b_k + Ac_k[U(\omega_z) \times \sqrt{(1-\omega_z^2)}\cos\Theta - T(\omega_z)\sin\Theta]\} \tag{18d}$$

$$C_2 = \sum_{k=0}^{n} \{U_k(\omega_z)\sqrt{(1-\omega_z^2)}d_k + Ae_k[U(\omega_z) \times \sqrt{(1-\omega_z^2)}\cos\Theta - T(\omega_z)\sin\Theta]\} \tag{18e}$$

$$D_2 = \sum_{k=0}^{n} \{U_k(\omega_z)\sqrt{(1-\omega_z^2)}f_k + Ag_k[U(\omega_z) \times \sqrt{(1-\omega_z^2)}\cos\Theta - T(\omega_z)\sin\Theta]\} \tag{18f}$$

In eqns. 18*a–f* the arguments ω_z, A and Θ have been omitted for simplicity. Setting $F(z, Ae^{-j\Theta}) = 0$, i.e. setting the real and imaginary parts of eqn. 17 equal to zero, yields

$$F_r = \alpha B_1 + \beta C_1 + D_1 = 0 \tag{19a}$$

$$F_i = \alpha B_2 + \beta C_2 + D_2 = 0 \tag{19b}$$

which are the two stability equations as defined in References 5, 6, 7 and 8. Solving eqns. 19*a* and *b* for α and β, one has

$$\alpha = \frac{C_1 \cdot D_2 - C_2 \cdot D_1}{\Delta} \tag{20a}$$

$$\beta = \frac{D_1 \cdot B_2 - D_2 \cdot B_1}{\Delta} \tag{20b}$$

where

$$\Delta = B_1 \cdot C_2 - B_2 \cdot C_1 \tag{21}$$

Let $A = 1$(0 dB) and $\Theta = 0$, and let ω_z vary from 1 to -1, then a stability boundary can be plotted in the α- vs. β-plane. Each point of this boundary can be considered as a condition for which the Nyquist plot of $G(z)$ passing through the critical point $(-1, j0)$, or at least a pair of characteristic roots, is on the unit circle of the z-plane. If A is assumed equal to a constant value and $\Theta = 0$, the curve in the parameter plane is the boundary of constant gain margin. On the other hand, if $A = 1$ and Θ is assumed equal to a constant value, a boundary of constant phase margin can be obtained. The corresponding

values of ω_z on the constant gain-margin boundary and constant phase-margin boundary are the phase crossover frequencies (ω_{zcp}) and the gain crossover frequencies (ω_{zcg}), respectively.

Since the relation between ω_z and ω is defined by

$$\omega_z = \cos \omega T \tag{22}$$

or

$$\omega = \frac{1}{T} \cos^{-1}(\omega_z) \tag{23}$$

It should be noted that the crossover frequencies represented by ω_z are quite different from the frequencies (ω) in the s-plane and that the variations of ω_z from 1 to -1 are equivalent to the variations of ω from $2m\pi/T$ to $(2m+1)\pi/T$, where $m = 0, 1, 2, \ldots$, due to the periodic strips in the s-plane.

Note also that, for the special cases such as $\omega_z = 1$ and/or $\omega_z = -1$, the substitutions of $z = \omega_z$ and $\Theta = 0$ into eqns. 13 and 14 yield

$$\alpha \sum_{k=0}^{n} (\omega_z)^k (b_k + c_k A) + \beta \sum_{k=0}^{n} (\omega_z)^k (d_k + e_k A) + \sum_{k=0}^{n} (\omega_z)^k (f_k + g_k A) = 0 \tag{24}$$

which may be represented by straight lines in the $\alpha\beta$-plane if ω_z and A are given. These straight lines can be considered as limits of stability boundaries and the constant gain-margin boundaries.

For analysis and design, one generally finds the stability boundary first, and then finds the boundaries of constant gain margin and phase margin that appear in the stable region. The method for determining the stable region by use of the stability boundary is that, if the sign of Δ defined in eqn. 21 is positive (negative), facing the direction in which the ω_z is decreasing, the left (right) side of the stability boundary is the stable region [3].

3 Examples

Example 1 [3]

Consider the system shown in Fig. 3, where the transfer functions are

$$G_1(s) = G_{ho}(s) = \frac{1 - e^{-Ts}}{s} \tag{25a}$$

$$G_2(s) = K \frac{s + h}{s + 0.01} \tag{25b}$$

$$G_3(s) = \frac{2.346}{(s + 2.3)(s + 0.51)} \tag{25c}$$

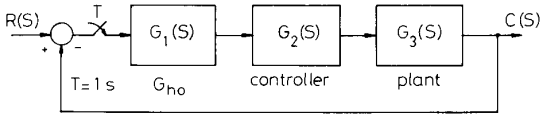

Fig. 3 *System block diagram of Example 1*

The purpose is to find all values of the parameters K and h which can make the system stable and have gain margin (GM) larger than 6 dB and phase margin (PM) in the range of $30° < PM < 60°$.

The open-loop transfer function in z-domain is given by

$$G(z) = K \frac{(0.24h + 0.51)z^2 + (0.43h - 0.28)z + (0.054h - 0.2)}{(z - 0.98)(z - 0.6)(z - 0.1)} \tag{26}$$

Letting $\alpha = Kh$ and $\beta = K$, the characteristic equation of the system with a gain-phase margin tester is

$$F(z, Ae^{-j\Theta}) = z^3 + (0.24Ae^{-j\Theta}\alpha + 0.51Ae^{-j\Theta}\beta - 1.68)z^2 + (0.43Ae^{-j\Theta}\alpha - 0.28Ae^{-j\Theta}\beta + 0.746)z + (0.054Ae^{-j\Theta}\alpha - 0.2Ae^{-j\Theta}\beta - 0.0588) = 0 \tag{27}$$

According to eqn. 14 and defining a coefficient vector $a_k = [b_k\ c_k\ d_k\ e_k\ f_k\ g_k]$, eqn. 27 gives

$$\begin{aligned} a_0 &= [0 \quad 0.054 \quad 0 \quad -0.20 \quad -0.0588 \quad 0] \\ a_1 &= [0 \quad 0.430 \quad 0 \quad -0.28 \quad 0.7460 \quad 0] \\ a_2 &= [0 \quad 0.240 \quad 0 \quad 0.51 \quad -1.6800 \quad 0] \\ a_3 &= [0 \quad 0.000 \quad 0 \quad 0.00 \quad 1.0000 \quad 0] \end{aligned} \tag{28}$$

Let $A = 1$, $\Theta = 0$. Using eqns. 18*a–f* and 20*a–b*, and letting ω_z change from 1^- to -1^+, a stability boundary can be plotted in the α- vs. β-plane as shown in Fig. 4.

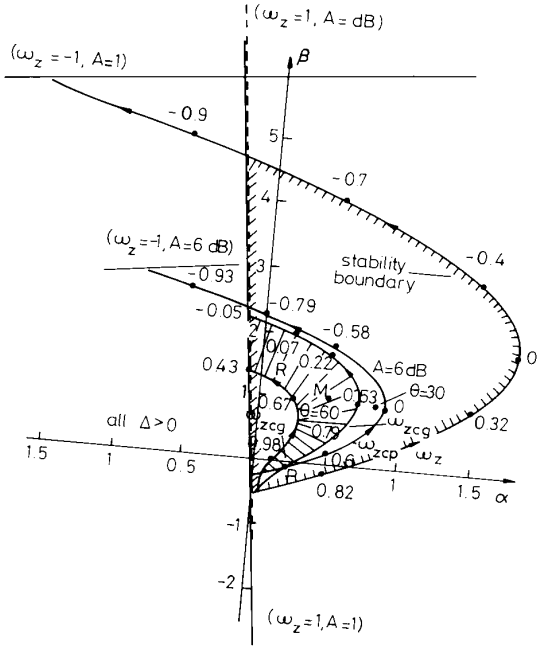

Fig. 4 *The boundaries of constant gain margin and constant phase margin in the α- vs. β-plane*

From eqn. 24, the equation for $\omega_z = 1$ and $\omega_z = -1$ are

$$0.724\alpha + 0.03\beta + 0.007 = 0 \quad \text{for } \omega_z = 1 \tag{29a}$$

$$0.136\alpha - 0.59\beta + 3.4548 = 0 \quad \text{for } \omega_z = -1 \tag{29b}$$

These two equations represent two straight lines which are shaded in accordance with the stability boundary to yield the stable region as indicated in Fig. 4.

Let $\Theta = 0°$ and $A = 6$ dB. Applying the same approach as before, the boundary of constant gain margin ($A = 6$ dB) can be obtained. The equations for the two straight lines are

$$0.724\alpha + 0.03\beta + 0.00351 = 0 \quad \text{for } \omega_z = 1 \tag{30a}$$

and

$$0.136\alpha - 0.59\beta + 1.74663 = 0 \quad \text{for } \omega_z = -1 \tag{30b}$$

then the region for $GM > 6$ dB in the stable region can be found. Similarly, by letting $A = 1$, $\Theta = 30°$ and $\Theta = 60°$, the two boundaries of constant phase margin can be obtained. Finally the region denoted by R for $GM > 6$ dB and $30° < PM < 60°$ as shown in Fig. 4 can be found.

In Fig. 4, if α and β are adjusted to point $P(0.2325, -0.0905)$, which is the intersection point of the boundaries of constant gain margin ($A = 6$ dB) and constant phase margin ($\Theta = 30°$), the system will have $GM = 6$ dB and $PM = 30°$. The corresponding phase crossover frequency ω_{zcp} and gain crossover frequency ω_{zcg} are at 0.832 and 0.932, respectively. By use of eqn. 23, the values of ω_{cp} and ω_{cg} are at 0.5881 rad/s and 0.371 rad/s, respectively. The results can be checked by use of Nyquist plot and Bode diagram as shown in Figs. 5A and B. In Fig. 4,

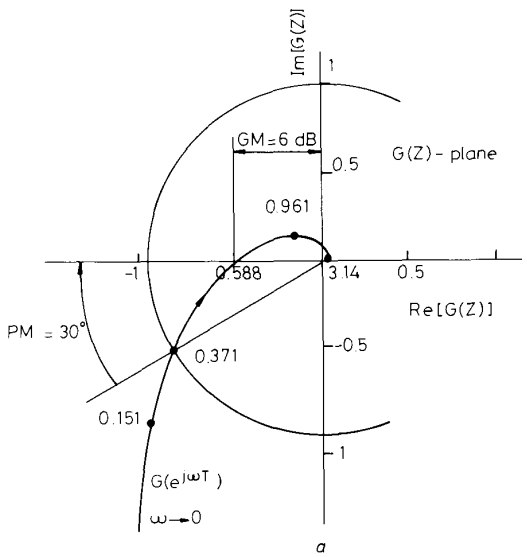

Fig. 5A *Nyquist plot of Example 1*

a point $M(\alpha, \beta) = (0.5, 1)$ has also been checked by use of Nyquist plot and Bode diagram, the results are: $GM = 9.51$ dB, $PM = 41.3°$, $\omega_{cp} = 1.971$ rad/s ($\omega_{zcp} = -0.3896$) and $\omega_{cg} = 0.935$ rad/s ($\omega_{zcg} = 0.6015$).

Example 2 [6, 9]

The block diagram of a high order proportional navigation system is shown in Fig. 6. Typical application of such a system is the missile homing system for engaging a moving target in the vertical plane. The seeker is a microwave or an IR (infra-red) device wth transfer function

$$\frac{V_r^*(s)}{\sigma^*(s)} = \frac{1}{K_a}\frac{\dot{\sigma}^*(s)}{\sigma^*(s)} = \left[G_{ho}\frac{K_r s(1 + 0.02s)}{K_a K_r + s(1 + 0.02s)}\right]^* \tag{31}$$

The combined transfer function of control system and vehicle dynamics is

$$\frac{\dot{\gamma}^*(s)}{V_r^*(s)} = \frac{G_{ho}G_1G_2G_3^*(s)}{1 + G_{ho}G_1G_2G_4^*(s) + G_{ho}G_1G_2G_3G_5^*(s)} \tag{32}$$

where the transfer functions of G_1, G_2, G_3, G_4, G_5 are shown in Fig. 6, and G_{ho} is the zero-order holding device. Assuming K_aK_r is equal to 15 and taking the z-

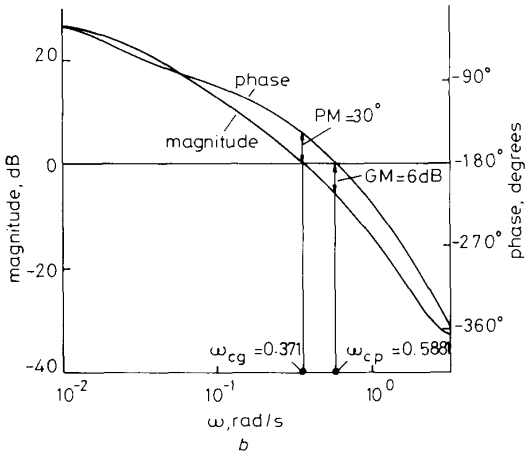

Fig. 5B *Bode diagram of Example 1*

transformation (for $T = 0.05$ s), eqns. 31 and 32 can be expressed, respectively, as

$$\frac{V_r(z)}{\sigma(z)} = \frac{1}{K_a}\frac{\dot{\sigma}(z)}{\sigma(z)} = \frac{K_r(z^2 - 0.9031z - 0.0969)}{z^2 - 0.4858z + 0.0821} \tag{33a}$$

and

$$\frac{\dot{\gamma}(z)}{V_r(z)} = \frac{-1.12K_s(-0.0936z^3 + 0.2552z^2 - 0.0979z + 0.0006)}{[(z^4 - 2.1743z^3 + 1.6214z^2 - 0.3584z + 0.0023) - 1.12K_sK_g(7.4668z^3 - 8.9718z^2 + 0.8598z + 0.7097) - 1.12K_sVK_{ac}(-0.0891z^3 + 0.232z^2 - 0.0718z + 0.0067)]} \tag{33b}$$

In order to ensure the proportional navigation constant N, it is required that the steady-state ratio of $\dot{\gamma}$ and $\dot{\sigma}$ be equal to N, i.e.

$$\left[\frac{\dot{\gamma}(z)}{\dot{\sigma}(z)}\right]_{z=1} = \frac{-1.12K_s}{K_a(1.414 - 1.12K_sK_g - 1.12K_sVK_{ac})} = N \tag{34}$$

The vehicle is considered as a point moving along its flight path with instantaneous displacements

$$dx = V\cos\gamma(t)\,dt \tag{35a}$$

$$dy = V\sin\gamma(t)\,dt \tag{35b}$$

where V is the velocity and γ is the flight-path angle.

The open-loop transfer function of the system can be considered as

$$G_o^*(s) = \frac{V_r^*(s)}{\sigma^*(s)} \times \frac{-G_{ho}\xi(t)s^{-1}G_1G_2G_3^*(s)}{1 + G_{ho}G_1G_2G_4^*(s) + G_{ho}G_1G_2G_3G_5^*(s)} \tag{36}$$

where $\xi(t)$ is a time-varying gain that represents the geometry relation. After the z-transformation, eqn. 36 can

be expressed as

$$G_o(z) = \frac{1.12K_r K_s \xi(t) X_1(z)}{X_2(z) - 1.12K_s K_g X_3(z) - 1.12K_s V K_{ac} X_4(z)} \quad (37)$$

where

$$X_1(z) = -3.0093 \cdot 10^{-3} z^5 + 5.331 \cdot 10^{-3} z^4 + 3.254 \cdot 10^{-3} z^3 - 1.8546 \cdot 10^{-3} z^2 - 1.9095 \cdot 10^{-4} z + 1.3698 \cdot 10^{-6} \quad (38a)$$

$$X_2(z) = z^6 - 2.6601 z^5 + 2.7598 z^4 - 1.3245 z^3 + 3.0953 \cdot 10^{-1} z^2 - 3.0555 \cdot 10^{-2} z + 1.9223 \cdot 10^{-4} \quad (38b)$$

$$X_3(z) = 7.4668 z^5 - 12.599 z^4 + 5.8311 z^3 - 4.4441 \cdot 10^{-1} z^2 - 2.7419 z + 5.8256 \cdot 10^{-2} \quad (38c)$$

$$X_4(z) = -8.9118 \cdot 10^{-2} z^5 + 2.7529 \cdot 10^{-1} z^4 - 1.9178 \cdot 10^{-1} z^3 + 4.7182 \cdot 10^{-2} z^2 - 2.6241 \cdot 10^{-3} z - 5.52 \cdot 10^{-4} \quad (38d)$$

The characteristic equation for the considered system with a gain-phase margin tester is

$$F(z, Ae^{-j\Theta}) = 1 + Ae^{-j\Theta} G_o(z) = X_2(z) - 1.12K_s K_g X_3(z) - 1.12K_s V K_{ac} X_4(z) + Ae^{-j\Theta} 1.12K_r K_s \xi(t) X_1(z) = 0 \quad (39)$$

Since $K_a K_r = 15$, letting

$$-1.12K_s K_g = \alpha \quad (40a)$$

$$-1.12K_s V K_{ac} = \beta \quad (40b)$$

eqn. 34 gives

$$1.12K_r K_s = -15N(1.414 + \alpha + \beta) \quad (41)$$

Substituting eqns. 40*a–b* and 41 into eqn. 37, and setting $z = 1$, the steady-state gain of the open-loop transfer function is

$$G_o(z)_{z=1} \approx -1.38\xi(t)N \quad (42)$$

which indicates that the steady-state gain of the system is proportional to $\xi(t)N$, and will not be affected by the parameters α and β. For system stability and the proportional navigation requirement, the condition is

$$\xi(t)N < 1/1.38 = 0.7246 \quad (43)$$

Substituting eqns. 40*a–b* and 41 into eqn. 39, the characteristic equation is

$$F(z, Ae^{-j\Theta}) = \alpha X_3(z) + \alpha Ae^{-j\Theta}[-15\xi(t)NX_1(z)] + \beta X_4(z) + \beta Ae^{-j\Theta}[-15\xi(t)NX_1(z)] + X_2(z) + Ae^{-j\Theta}[-15\xi(t)N \times 1.414X_1(z)] = \sum_{k=0}^{6} a_k(z)z^k = 0 \quad (44)$$

which shows that, if $\xi(t)N$ is given, the coefficient vector a_k can be obtained directly from the coefficients of eqns. 38*a–d*. Assuming $\xi(t)N = 0.6$, the stability boundary, and the boundaries of constant gain margins ($A = 10$ dB, $A = -10$ dB, $A = -\infty$ dB) and phase margins ($\Theta = 45°$, $\Theta = -45°$) are plotted in the α- vs. β-plane as shown in Fig. 7. It can be seen that the boundaries of constant gain margins and phase margins of both positive, and negative signs appear in the stable region. This is because the system has an unstable open-loop zero, and the parameters α and β may yield unstable open-loop poles for the system. Note that the region in the right-hand side of the boundary for $A = -\infty$ dB will give the system a positive gain margin, which means that the open-loop transfer function of the system has stable poles.

On the other hand, the region in the left-hand side of the boundary for $A = -\infty$ dB will give the system positive as well as negative gain margins, and the open-loop transfer function has unstable poles. For example, if α and β are adjusted to point $P_1(\alpha = 0.1, \beta = 3.35)$, the

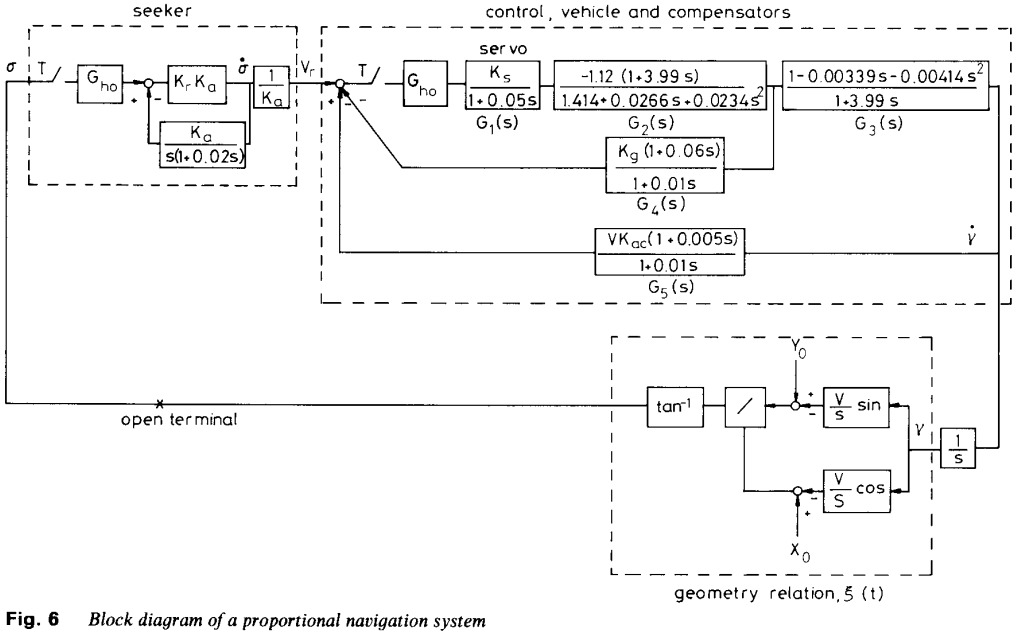

Fig. 6 *Block diagram of a proportional navigation system*

open-loop transfer function is

$$G_o(z) = \frac{0.1317(z - 0.0067)(z + 0.0969) \times (z - 0.4504)(z + 0.7249)(z - 2.1361)}{(z - 0.1652)(z - 0.3910)(z - 0.585 \pm j0.6662)(z - 0.2429 \pm j0.1519)} \quad (45)$$

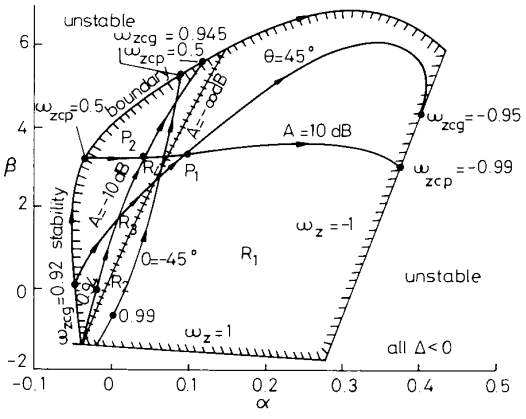

Fig. 7 *The boundaries of constant gain margin and phase margin of Example 2*

which has a zero at 2.1361 outside the unit circle. If α and β are adjusted to point $P_2(\alpha = 0.044, \beta = 3.22)$, the open-loop transfer function is

$$G_o(z) = \frac{0.1267(z - 0.0067)(z + 0.0969) \times (z - 0.4504)(z + 0.7249)(z - 2.1361)}{(z - 0.0235)(z - 0.4145)(z - 0.8474 \pm j0.710)(z - 0.2429 \pm j0.1519)} \quad (46)$$

which has a zero at 2.1361 and a pair of unstable poles at $0.8474 \pm j0.710$. The Nyquist plots and the Bode diagrams of eqns. 45 and 46 are shown in Figs. 8A, B and C,

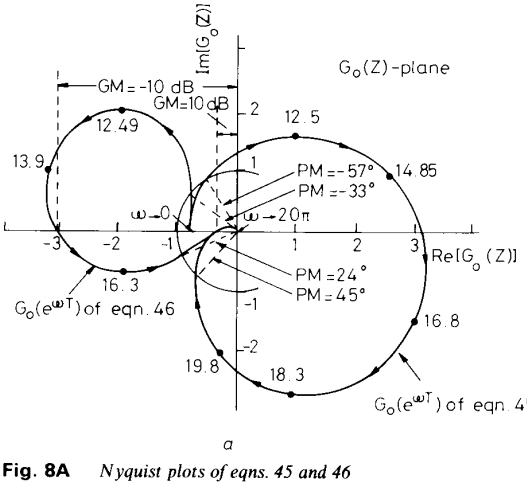

a

Fig. 8A *Nyquist plots of eqns. 45 and 46*

which indicate that the results for gain margins and phase margins are the same as those given in Fig. 7.

From Figs. 7 and 8 it can be seen that, for analysis and design of a system with adjustable parameters, to plot the boundaries of constant gain margin and phase margin is better than plotting several Nyquist plots and Bode diagrams. Since one generally finds the stable region first and then finds the boundaries of constant gain margin and phase margin that appear in the stable region, one does not need to worry about the signs of the

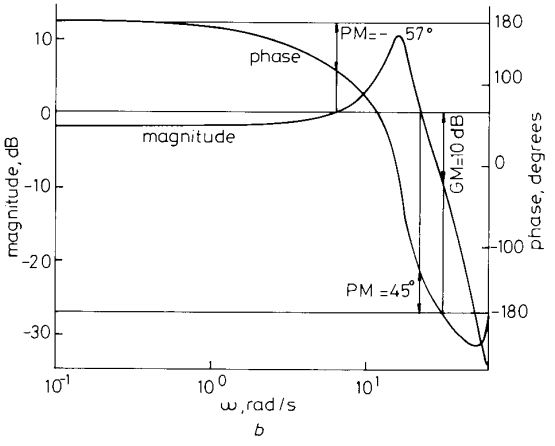

b

Fig. 8B *Bode diagram of eqn. 45*

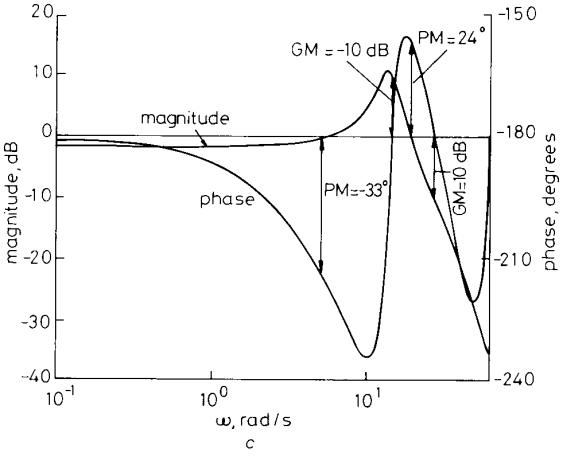

c

Fig. 8C *Bode diagram of eqn. 46*

gain margin and phase margin to represent the relative stability of the system.

In addition, the stable region is separated into several regions by the boundaries of constant gain margin and constant phase margin, and each region has its specified characteristics on gain margin and phase margin. For example, the region marked by R_1 will give $GM > 10$ dB, $PM > 45°$ and $PM < -45°$; the region marked by R_2 will give $GM > 10$ dB, $PM > 45°$ and $PM > -45°$; the region marked by R_3 will give $GM > 10$ dB, $GM < -10$ dB, $PM > 45°$ and $PM > -45°$; the region marked by R_4 will give $GM > 10$ dB, $GM < -10$ dB, $PM < 45°$ and $PM > -45°$. In short, a designer can select desirable values of parameters to make the system meet specifications on gain margin and phase margin simply by looking at a few boundaries.

In order to find the effects of the third parameter $\xi(t)N$, several values are assigned to it, and the corresponding boundaries in parameter planes are found. Then, a subspace with $A = -\infty$ dB, $A = 25$ dB, $\Theta = -45°$ and $\Theta = -90°$ in a three-dimensional parameter space can be constructed as shown in Fig. 9. Inside this subspace any point selected will represent a set of values of α, β and $\xi(t)N$ to make the system meet specifi-

cations $GM > 25$ dB and $-90° < PM < -45°$. For testing purposes, three points (Q_1, Q_2, Q_3) in the subspace are selected, a unit impulse disturbance at σ is assumed, and the responses at σ are obtained as shown in Fig. 10.

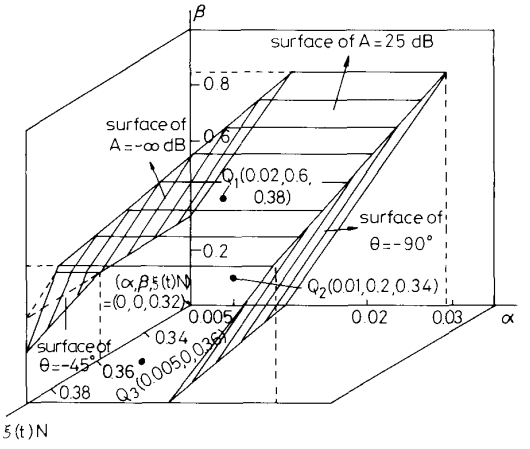

Fig. 9 *A subspace for $GM > 25$ dB and $-90° < PM < -45°$*

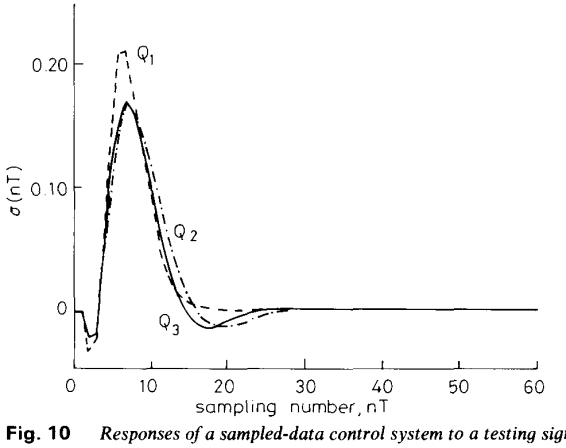

Fig. 10 *Responses of a sampled-data control system to a testing signal*

Note that since N is the proportional navigation constant which is preselected, such as $N = 2$, the third parameter is $\xi(t)$ instead of $\xi(t)N$. Since $\xi(t)$ is time varying, all the characteristics of the system, such as gain margin, phase margin and crossover frequencies, are time varying. Therefore, a designer must first define the range of $\xi(t)$ from the geometry relation as shown in Fig. 6, then check the ranges of variations of gain margins, phase margins and crossover frequencies, and finally the proper values of parameters (α and β) can be defined by use of the subspace as shown in Fig. 9.

In short, the presented method is useful for analysis and design of control systems with adjustable and/or variable parameters. It is more useful than the commonly used methods, such as Bode diagram and Nyquist plot, especially for the complicated system as shown in Example 2, which has multiple gain margins and phase margins.

4 Conclusions

A method for finding the boundaries of constant gain margin and phase margin of sampled-data control systems with adjustable parameters has been presented. The relations among gain margins, phase margins and adjustable parameters can be defined completely and easily.

From the two examples, it can be seen that, by use of the presented method, the works of analysis and design of sampled-data control systems with adjustable parameters to meet specifications on gain margins and phase margins and their corresponding crossover frequencies can be much simplified by looking at a few boundaries in a parameter-plane or a parameter-space.

Since all the analyses are based upon two stability equations, and all the calculations are performed in the real domain, the presented method has the potential for analysis and design of very complicated sampled-data control systems.

5 References

1 HOROWITZ, I.: 'Quantitative feedback theorey', *IEE Proc. D, Control Theory & Appl.*, 1982, **129,** (6), pp. 215–226
2 AIZERMAN, M.A.: 'Theory of automatic control' (Pergamon Press, 1963), pp. 163–170
3 ŠILJAK, D.D.: 'Analysis and synthesis of feedback control system in the parameter plane', *IEEE Trans.*, 1964, **AI-83,** pp. 449–473
4 SELTZER, S.M., ASNER, B.A., and JACKSON, R.L.: 'Parameter-plane analysis for large-scale systems', *AIAA J. Guidance*, 1982, **5,** (2), pp. 158–163
5 HAN, K.W., and THALER, G.J.: 'High order system analysis and design using the root locus method', *J. Franklin Inst.*, 1966, **281,** (2), pp. 99–113
6 WANG, L.C., and HAN, K.W.: 'Analysis of sampled-data control systems by stability-equation method', *ibid.*, 1978, **306,** (1), pp. 87–106
7 CHANG, C.H., and HAN, K.W.: 'Gain margins and phase margins for control systems with adjustable parameters', *AIAA J. Guidance*, accepted for publication
8 CHANG, C.H., and HAN, K.W.: 'Gain margin and phase margin analysis of a nuclear reactor control system with multiple transport lags', *IEEE Trans.*, 1989, **NS-36,** (4), pp. 1418–1425
9 HAN, K.W.: 'Digital and sampled-data control systems' (Kuang-Mei Publishing Co., Lungtan, Taiwan, 1979), pp. 307–314